Mon. Not. R. Astron. Soc. **000**, 1–9 (2016) Printed March 7, 2016 (MN LATEX style file v2.2)

New numerical integration of orbits of irregular satellites and prediction of stellar occultations up to 2020

A. R. Gomes-Júnior[1⋆], M. Assafin[1,†], L. Beauvalet[2,3], J. Desmars[4], R. Vieira-Martins[1,2,5,†], J. I. B. Camargo[2,5], B. E. Morgado[1,2] F. Braga-Ribas[2,6]

[1] *Observatório do Valongo/UFRJ, Ladeira Pedro Antônio 43, CEP 20.080-090 Rio de Janeiro - RJ, Brazil*
[2] *Observatório Nacional/MCTI, R. General José Cristino 77, CEP 20921-400 Rio de Janeiro - RJ, Brazil*
[3] *Observatoire de Paris/SYRTE, 77 Avenue Denfert Rochereau 75014 Paris, France*
[4] *Institut de mécanique céleste et de calcul des éphémérides - Observatoire de Paris, UMR 8028 du CNRS, 77 Av. Denfert-Rochereau, 75014 Paris, France*
[5] *Laboratório Interinstitucional de e-Astronomia - LIneA, Rua Gal. José Cristino 77, Rio de Janeiro, RJ 20921-400, Brazil*
[6] *Federal University of Technology - Paraná (UTFPR / DAFIS), Rua Sete de Setembro, 3165, CEP 80230-901, Curitiba, PR, Brazil*

Accepted . Received ; in original form

ABSTRACT

Due to their orbital configurations, it is common belief that the irregular satellites were probably captured by the giant planets in the early solar system. It is important to know their physical parameters, such as size, shape, albedo and composition, to trace back their true origin. The best ground-based technique to determine size and shape, and thus constrain the albedo and in a broader sense composition, is the observation of stellar occultations by these objects. We aim to predict stellar occultations for the eight largest irregular satellites of Jupiter: Himalia, Elara, Pasiphae, Carme, Lysithea, Sinope, Ananke and Leda, and for the irregular satellites Phoebe of Saturn and Nereid of Neptune, and also for Triton. We identified candidates to stellar occultations by the irregular satellites from the UCAC4 catalogue and from a catalogue of stars in the sky-path of Neptune obtained from observations made with the ESO2p2/WFI (2.2 m Max-Planck ESO telescope with the Wide Field Imager) instrument. These catalogues were crossed with the ephemeris of the satellites to identify stellar occultations. We used a new ephemeris based solely on the observations from Gomes-Júnior et al. (2015) to generate predictions for the short-time future of the satellites of Jupiter. For Phoebe, we used an updated ephemeris and for Nereid and Triton we used recently published ephemeris. We managed to identify 5457 candidates of stellar occultations between the period of January, 2016 and December, 2020. We made observational tests for the prediction of the event of Himalia in March 03, 2015. The stars and objects were observed close to the date predicted and in the same field to minimize errors and the obtained relative satellite-star positions were used to evaluate the predictions. The comparisons between the predictions and the observation tests show a good agreement. We call attention for an occultation by Triton of a bright star (R=12.5) in October 5, 2017. The event can be observed from Europe and the east coast of USA and will be a good opportunity to access the current state of the atmosphere of the satellite. We also note that Jupiter will cross the galactic plane in 2019-2020 and Saturn in 2018. This results in a large number of occultations predicted for that period. We discuss how the successful observation of a stellar occultation by these objects is quite possible and present some of those potential occultations.

Key words: occultations - planets and satellites: general - planets and satellites: individual: Jovian and Saturnian irregular satellites - planets and satellites: individual: Triton

1 INTRODUCTION

Irregular satellites revolve around giant planets at large distances in eccentric, highly inclined and frequently retrograde

⋆ E-mail: altair08@astro.ufrj.br

orbits. Because of these peculiar orbits, it is largely accepted that these objects did not form by accretion around their planet, but were captured in the early solar system (Sheppard 2005).

There is no consensus for a single model explaining where the irregular satellites were formed. Ćuk & Burns (2004) showed that the progenitor of the Himalia group may have originated in heliocentric orbits similar to the Hilda asteroid group. Sheppard (2005) stated that the irregular satellites may be some of the objects that were formed within the giant planets region.

Grav et al. (2003) and Grav & Bauer (2007) showed that the irregular satellites from the giant planets have their colors and spectral slopes similar to C-, D- and P-type asteroids, Centaurs and trans-neptunian objects (TNOs). This suggests that they may have come from different locations in the early solar system.

Sheppard (2005) and Jewitt & Haghighipour (2007) also explored the possibility that the irregular satellites originated as comets or TNOs. TNOs are highly interesting objects that, due to their large heliocentric distances, may be highly preserved with physical properties similar to those they had when they were formed (Barucci et al. 2008). This is even more true for the smaller objects, since in principle larger sizes favour physical differentiation processes in the body and vice-versa. However, due to the distance, the smaller TNOs from this region are more difficult to observe. Thus, if irregular satellites - or at least a few of them - do share a common origin with small TNOs, and since these objects are situated at much closer heliocentric distances now, this gives a unique chance of observing and studying representatives of this specific TNO population in much greater detail than could ever be possible by direct observation of this population in the Kuiper Belt.

Phoebe is the most studied irregular satellite. Clark et al. (2005) suggest that its surface is probably covered by material of cometary origin. It was also stated by Johnson & Lunine (2005) that if the porosity of Phoebe is 15%, Phoebe would have an uncompressed density similar to those of Pluto and Triton.

In order to obtain precise fundamental physical parameters like size and shape, thus constraining the albedo and in a broader sense also the composition for the irregular satellites and therefore to contribute to the study of their origin, we aim at observing stellar occultations, which provide more accurate results than other ground-based techniques (Sicardy et al. 2011; Ortiz et al. 2012; Braga-Ribas et al. 2014). For that, reliable predictions of stellar occultations by these satellites are most needed.

We present in this paper new numerical integration of the orbits of the 8 major irregular satellites of Jupiter (Himalia, Elara, Pasiphae, Lysithea, Carme, Ananke, Sinope and Leda) for predict stellar occultations. This is a specific short-time ephemeris using only the positions obtained by Gomes-Júnior et al. (2015). Gomes-Júnior et al. (2015) obtained 6523 suitable positions for 18 irregular satellites between 1992 and 2014 with an estimated error in the positions of about 60 to 80 mas. For some satellites the number of positions obtained is comparable to the number used in the numerical integration of orbits by the JPL (Jacobson et al. 2012). They pointed out that the ephemeris of the irregular satellites have systematic errors that may reach 200 mas for some satellites. For an object at the distance of Jupiter, this represents an error langer than 700 km in the shadow path of an occultation.

For Phoebe, we updated the ephemeris of Desmars et al. (2013) using the observations of Gomes-Júnior et al. (2015), observations from Minor Planet Center and observations from Flagstaff. For Nereid and Triton we used the most recent ephemeris available.

Also, with new and precise ephemeris, we present stellar occultation predictions for these 11 objects up to 2020. Phoebe, being the most studied object with a good measured size, can be used to calibrate and evaluate the technique for similar objects.

Triton is an uncommon satellite. Its orbit is retrograde and inclined, but quasi-circular and very close to the planet compared to the irregular ones. Because Triton's orbit size is very small and its precession is not dominated by Solar perturbations, Triton is frequently excluded from the irregular satellites' class, but still studied together by many authors (Sheppard 2005; Jewitt & Haghighipour 2007). Similarly to the irregular satellites, Triton was probably captured in the early solar system and may have the same origin as the TNOs (Agnor & Hamilton 2006). However, Triton is bigger than the irregular satellites by an order of magnitude and has an atmosphere. The main motivation to study Triton by stellar occultations is to understand the evolution of its atmosphere due to Triton's complicated and extreme seasonal cycle (McKinnon & Kirk 2007; Elliot et al. 2000). For all these reasons, Triton was also included as a target in this work.

Excluding Triton (Olkin et al. 1997; Elliot et al. 2000), no observation of a stellar occultation by an irregular satellite was published up to date. Since their estimated sizes are very small (see Table 1), this may have discouraged earlier tries. But, in fact, given their relatively closer distances as compared to TNOs and Centaurs, and considering the current precision of their ephemeris and of star positions, we can now reliably predict the exact location and instant where the shadow of the occultation will cross the Earth. For instance, Himalia, supposedly the largest irregular satellite of Jupiter has an estimated size of 150 km (Porco et al. 2003), which is equivalent to an apparent size of about 40 mas (milliarcseconds). Thus, in this case, if the accumulated error (2 sigma or 95% confidence level) of ephemeris and star position be around 70 mas, we have a probability of about 30% of observing a stellar occultation, which is quite satisfactory today (see discussion in section 4).

Since 2009 many successful observations of stellar occultations by TNOs have been reported in the literature (Elliot et al. 2010; Sicardy et al. 2011; Ortiz et al. 2012; Braga-Ribas et al. 2013), the main disadvantages in their prediction being large heliocentric distances and ephemeris error, facts somewhat compensated for the larger diameters involved. In contrast to TNOs, the irregular satellites have much better ephemeris because the orbits of their host planets are better known, their observational time span is much wider and covers many orbital periods. Moreover, the irregular satellites are much closer to Earth which implies in a much smaller shadow path error in kilometers. These advantages may be somewhat balanced by the smaller sizes estimated for the irregular satellites.Thus, in comparison, the chances for a successful observation of an stellar occul-

Table 1. Estimated diameter of the satellites and correspondent apparent diameter

	Diameter of the satellites		
Satellite	mas[a]	km	Ref.
Ananke	8	29	1
Carme	13	46	1
Elara	24	86	1
Himalia	41	$(150 \times 120) \pm 20^b$	2
Leda	5	20	1
Lysithea	10	36	1
Pasiphae	17	62	1
Sinope	10	37	1
Phoebe	32	212 ± 1.4^b	3
Nereid	15	340 ± 50^c	4
Triton	124	2707 ± 2.0^c	5

References: (1) Rettig et al. (2001); (2) Porco et al. (2003); (3) Thomas (2010); (4) Thomas et al. (1991); (5) Thomas (2000).
[a]Using a mean distance from Jupiter of 5 AU, from Saturn of 9 AU and from Neptune of 30 AU. [b]From Cassini observations. [c]From Voyager-2 observations.

tation by an irregular satellite should be considered at least also as good as those by TNOs.

In section 2 we show the building of the new ephemeris. In section 3, we present the predictions of the stellar occultations by irregular satellites and how they were made. Some tests made to check the accuracy of the predictions are presented in section 3.1 and the final discussion is presented in section 4.

2 EPHEMERIS

In order to improve ephemeris in short time spans in the near future for a more efficient prediction of stellar occultations by irregular satellites, we need predictions based on new and recent observations. In this context, Gomes-Júnior et al. (2015) published 6523 precise positions for 18 irregular satellites from observations made at the Observatório do Pico dos Dias (OPD), Observatoire Haute-Provence (OHP) and European Southern Observatory (ESO) between 1992 and 2014.

Here we develop our own ephemeris based on the observations published in Gomes-Júnior et al. (2015). First, because the reduction was made with consistent and precise stellar catalogue and with a robust and reliable software (PRAIA, Assafin et al. 2011). Second, besides recent observations, this consistent set of numerous and precise positions covers many orbital periods at many distinct orbital plane sights, so that the orbital inclinations along with all other orbital elements could be satisfactorily derived without the need of further position sets. For these reasons, only this set of positions was used for building the new ephemeris for the satellites of Jupiter.

2.1 Special tailored Ephemerides (STE) for Jupiter irregular satellites

The last observations used to develop JPL current ephemeris of the irregular satellites of Jupiter were obtained in 2012 (Jacobson et al. 2012). As a result, the errors in the JPL ephemeris for the current epoch are large enough to prevent accurate predictions of stellar occultations without any corrections.

Our numerical model describes the dynamical evolution of the irregular satellites of Jupiter in a jovicentric reference frame. The satellites are submitted to the influence of the Sun and the rest of the solar system, as well as that of the Galilean satellites and the first harmonics of Jupiter's gravity field. The axes of the reference frame are those of the ICRS.

We use the following notations:

- i and l one of the irregular satellites of Jupiter
- J Jupiter
- j another body of the Solar System
- M_j the mass of the j-th body, not an irregular satellite
- m_i the mass of the irregular satellite i
- $\vec{r_i}$ the position of the i-th body with respect to the barycentre of Jupiter System
- r_{ij} the distance between bodies i and j
- R_J the radius of Jupiter
- J_n the dynamic polar oblateness of the n-th order for Jupiter's gravity field
- $U_{\bar{l}\hat{J}}$ potential generated by the oblateness of Jupiter on the satellite l
- Φ_i is the inclination of the i-th satellite with respect to Jupiter's equator.

For an irregular satellite i, under the gravitational influence of Jupiter, the $\mathcal{N}-1$ other irregular satellites, the regular Jovian satellites and the rest of the Solar System ($\mathcal{N}$ bodies), the equation of motion is:

$$\begin{aligned}\ddot{\vec{r_i}} = \; & -GM_J\frac{\vec{r_J}-\vec{r_i}}{r_{iJ}^3} - \sum_{l=1,l\neq i}^{\mathcal{N}'} Gm_l\frac{\vec{r_l}-\vec{r_i}}{r_{il}^3} \\ & -\sum_{j=1}^{\mathcal{N}} GM_j\left(\frac{\vec{r_j}-\vec{r_i}}{r_{ij}^3} - \frac{\vec{r_j}-\vec{r_J}}{r_{Jj}^3}\right) \\ & +GM_J\nabla U_{\bar{l}\hat{J}} - \sum_{l=1}^{\mathcal{N}} Gm_l\nabla U_{\bar{l}\hat{J}}\end{aligned} \quad (1)$$

where the last term in the brackets and the last term in Eq. 1 represent undirect perturbations. The oblateness potential seen by the body i because of Jupiter is:

$$\begin{aligned}U_{\bar{l}\hat{J}} = \; & -\frac{R_J^2 J_2}{r_{iJ}^3}\left(\frac{3}{2}\sin^2\Phi_i - \frac{1}{2}\right) \\ & -\frac{R_J^4 J_4}{r_{iJ}^5}\left(\frac{35}{8}\sin^4\Phi_i - \frac{15}{4}\sin^2\Phi_i + \frac{3}{8}\right) \\ & -\frac{R_J^6 J_6}{r_{iJ}^7}\left(\frac{231}{16}\sin^6\Phi_i - \frac{315}{16}\sin^4\Phi_i + \frac{105}{16}\sin^2\Phi_i - \frac{5}{16}\right)\end{aligned} \quad (2)$$

The expressions of $\nabla_l U_{\bar{l}\hat{i}}$ and $\nabla_i U_{\bar{i}\hat{l}}$. have been developed in Lainey et al. (2004). The equations of motion are integrated with the numerical integrator RADAU (Everhart 1985). Our model was fitted to the observations through a least-squares procedure. The satellites were integrated one dynamical family at a time, to gain computing time, while losing minimum precision. Indeed, the interactions between satellites not belonging to the same dynamical family are negligible considering the short timespan of our integration.

Table 2. Initial osculating elements for Jupiter irregular satellites at JD 2451545.0.

Satellite	a (km)	e	I°	Ω°	ω°	v°
Himalia	11372100 ± 500	0.166 ± 0.002	45.14 ± 0.15	39.77 ± 0.19	351.48 ± 0.46	97.35 ± 0.48
Elara	11741170 ± 690	0.222 ± 0.002	28.64 ± 0.18	68.42 ± 0.43	179.82 ± 0.56	339.08 ± 0.82
Lysithea	11739900 ± 1300	0.136 ± 0.004	51.12 ± 0.27	5.53 ± 0.52	53.0 ± 1.5	318.9 ± 2.0
Leda	11140300 ± 4300	0.173 ± 0.007	16.15 ± 0.75	272.6 ± 1.7	212.2 ± 3.6	218.8 ± 3.2
Pasiphae	23425000 ± 5000	0.379 ± 0.001	152.44 ± 0.10	284.59 ± 0.21	135.96 ± 0.19	236.97 ± 0.16
Sinope	22968800 ± 5200	0.316 ± 0.002	157.76 ± 0.12	256.62 ± 0.55	298.38 ± 0.55	167.57 ± 0.19
Carme	24202924 ± 4800	0.242 ± 0.001	147.13 ± 0.10	154.01 ± 0.25	47.90 ± 0.29	234.41 ± 0.19
Ananke	21683800 ± 7200	0.380 ± 0.002	172.29 ± 0.20	56.9 ± 1.2	123.3 ± 1.2	231.24 ± 0.21

Notes: a: semimajor axis; e : excentricity; I: inclination relative to the equatorial reference plane J2000; Ω: longitude of the ascending node; ω: argument of periapsis; v: true anomaly.

The initial osculating elements at the origin of integration are presented in Table 2.

All the orbits determined for the satellites show satisfying residuals. The residuals are smaller than those obtained with JPL ephemeris, which was expected because the accuracy of an ephemeris decreases when we get further from the time of observations. The main risk of divergence over time comes from the possible absence of long-term effects when fitting to a short timespan of observations. If that were the case, our ephemeris would diverge too quickly to be of any use. JPL ephemerides are fitted over all the available observations. As a result, they will diverge less quickly than our own. Though they are no longer precise enough for our use, they remain a precious reference to identify whether our own model presents a quick divergence.

We compared our ephemeris to the JPL for all the Jupiter satellites we fitted, until 2018. For instance, the divergence between 2015 and 2018 is at most 98 mas in $\Delta\alpha\cos\delta$ and 58 mas in $\Delta\delta$ for Himalia and 181 mas in $\Delta\alpha\cos\delta$ and 152 mas in $\Delta\delta$ for Carme.

Fig. 1 displays the offsets of the positions published by Gomes-Júnior et al. (2015) for the satellite Carme in declination relative to our ephemeris, to Jacobson et al. (2012) JUP300 JPL ephemeris and Emel'yanov & Arlot (2008) ephemeris.We see that the systematic JPL ephemeris offsets pointed out by Gomes-Júnior et al. (2015) are reduced with our ephemeris, as expected.

The obtained ephemeris is hereafter refered as STE, for special-tailored ephemeris.

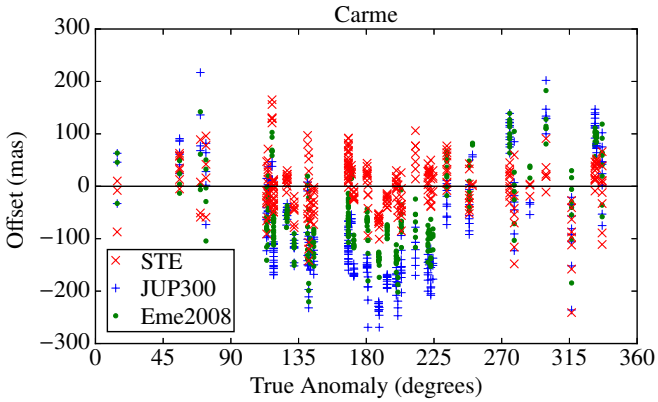

Figure 1. Offsets in declination of the positions published by Gomes-Júnior et al. (2015) for Carme. The red "x" relative to the special-tailored ephemeris, the blue "+" relative to the JUP300 JPL ephemeris and the green dot relative to Emel'yanov & Arlot (2008). As expected, the ephemeris systematic errors pointed out by Gomes-Júnior et al. (2015) are reduced with the STE ephemeris.

2.2 Phoebe's ephemeris

For the specific case of Phoebe, the ninth satellite of Saturn, we have updated the ephemeris published in Desmars et al. (2013). The new ephemeris (PH15) used the same dynamical model, including the perturbations of the Sun and the eight planets, the eight major satellites of Saturn and the J_2 parameter. The observations used to fit the model are identical to Desmars et al. (2013) (including 223 Cassini observations) with additional observations from Gomes-Júnior et al. (2015), Peng et al. (2015), observations from Minor Planet Circulars between 2012 and 2014 (available on the Natural Satellite Data Center[1]), and observations from Flagstaff (U.S.N.O 2015) between 2012 and 2014. It represents a total number of 5886 observations from 1898 to 2014.

In Fig. 2 we compare our ephemeris (PH15) with the SAT375 JPL[2] ephemeris. The difference between them is smaller than 30 mas (< 10 mas in Declination). This difference is smaller than the apparent diameter of Phoebe (see Table 1)

2.3 Triton's and Nereid's ephemeris

For Triton, we used the most recent ephemeris published by Emelyanov & Samorodov (2015). In Fig. 3 we compare it with the ephemeris published in Zhang et al. (2014) and the NEP081 JPL ephemeris (Jacobson 2009). The offsets between the three ephemeris are smaller than 15 mas for the period 2015-2018. This value is much smaller than the apparent size of Triton (124 mas, see Table 1), which indicates a good probability of observing an event by this object.

[1] `http://lnfm1.sai.msu.ru/neb/nss/bsapoouf.htm`

[2] Jacobson, R.A. 2015-Feb-27. "Satellite Ephemeris: SAT375", JPL Satellite Ephemeris File Release, `ftp://ssd.jpl.nasa.gov/pub/eph/satellites/nio/LINUX_PC/sat375l.txt`

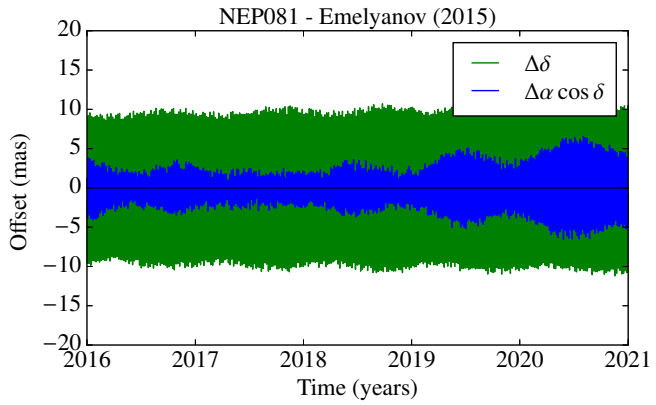

(a) NEP081 JPL and Emelyanov & Samorodov (2015)

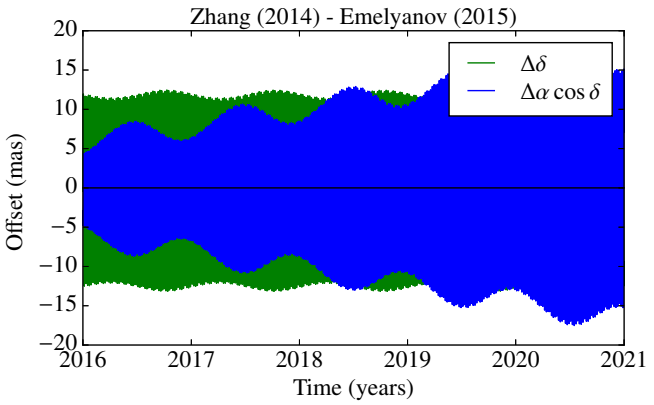

(b) Zhang et al. (2014) and Emelyanov & Samorodov (2015)

Figure 3. Comparison between the Emelyanov & Samorodov (2015), Zhang et al. (2014) and NEP081 JPL (Jacobson 2009) ephemeris for the satellite Triton.

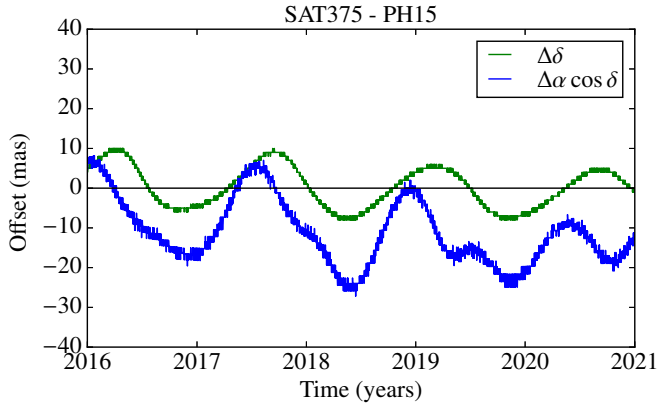

Figure 2. Comparison between the PH15, SAT375 JPL and Planet & Observations (Eme) ephemeris for the satellite Phoebe.

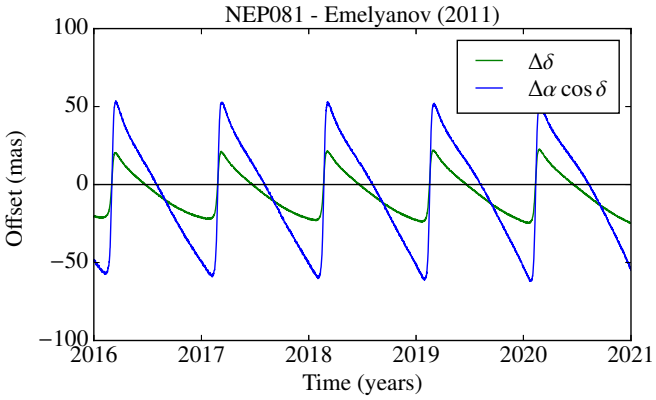

Figure 4. Comparison between the Emelyanov & Arlot (2011) and NEP081 JPL (Jacobson 2009) ephemeris for the satellite Nereid.

For Nereid, we used the ephemeris published by Emelyanov & Arlot (2011), which uses more recent observations than the JPL ephemeris published by Jacobson (2009). The comparison between the two ephemeris can be seen in Fig. 4. The right ascension offsets between them are smaller than 60 mas and the declination ones are smaller than 15 mas. For Nereid, ephemeris errors in right ascension translate to uncertainties in the central instant of a stellar occultation, so offsets of 60 mas are not critical. The declination ephemeris offsets are of the order of the apparent diameter (15 mas, see Table 1), resulting in fair chances (50%) that the shadow crosses the expected Earth latitude predicted for an occultation.

Gomes-Júnior et al. (2015) published 902 new positions for Nereid from observations between 1992 and 2014. The development of a better ephemeris for Nereid using these new positions in the context discussed here of near future stellar occultations is desirable, but is out of the scope of this paper.

3 PREDICTION OF OCCULTATIONS

The prediction of the occultations was made by crossing the stellar coordinates and proper motions of the UCAC4 catalogue (Zacharias et al. 2013) with the ephemeris presented in Sec. 2. The search for stellar candidates follows the same procedure as presented by Assafin et al. (2010, 2012) and Camargo et al. (2014).

We predicted occultations for the 8 major irregular satellites of Jupiter, Ananke, Carme, Elara, Himalia, Leda, Lysithea, Pasiphae and Sinope, and for Phoebe of Saturn and Triton and Nereid of Neptune.

For Triton and Nereid, the candidates for stellar occultations in 2016 were searched using the WFI catalogue in the same way as the predictions for Centaurs and TNOs occultations by Assafin et al. (2010, 2012) and Camargo et al. (2014). This catalogue contains the stars in the path of Neptune in the sky up to mid-2016. The catalogue was generated by observations made at the ESO 2p2 telescope (IAU code 809) using the Wide Field Imager (WFI) CCD mosaic detector. The filter used was the broad-band R filter ESO#844 with $\lambda_c = 651.725$ nm and $\Delta\lambda = 162.184$ nm.

A total of 5457 events were identified between January

Table 3. Number of stellar occultations for each satellite from January, 2016 up to December, 2020.

Satellite	2016	2017	2018	2019	2020	Total
Ananke	12	16	49	359	187	623
Carme	20	14	30	369	220	653
Elara	14	16	33	305	193	561
Himalia	15	12	54	257	230	568
Leda	8	24	38	362	208	640
Lysithea	16	11	35	330	212	604
Pasiphae	20	19	44	362	206	651
Sinope	15	21	34	356	256	682
Phoebe	32	98	238	79	13	460
Nereid	11[a]	1	1	0	0	13
Triton	–	1	1	0	0	2

[a] Using the WFI catalogue as explained in Sec. 3.

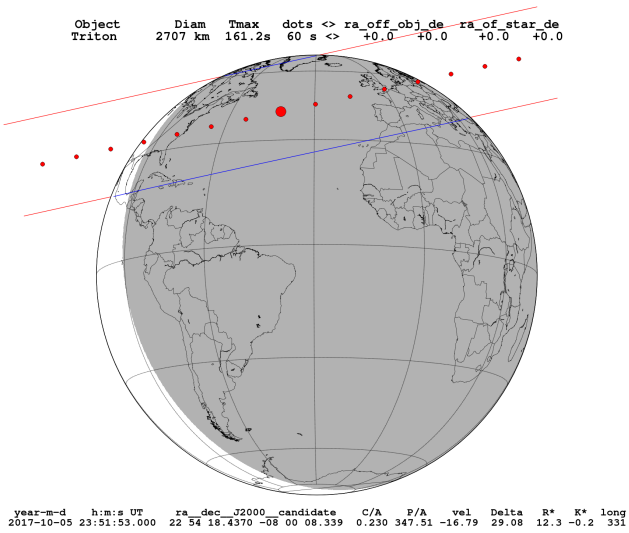

Figure 5. Occultation map for Triton.The central red dot show the geocentric closest approach of the shadow. The small ones shows the center of the shadow separated by 60s. The lines show the path of the shadow over the Earth. The shadow moves from right to left. **Labels:** Diam: Diameter of the object; Tmax: Maximum duration of the event for a central observation; C/A: the geocentric closest approach, in arcseconds; P/A: the satellite position angle with respect to the occulted star at C/A, in degrees; vel: velocity of event in km/s; Delta: Geocentric distance to the occulting object in AU; R^*: normalized magnitude to a common shadow velocity of 20 km s^{-1}; long: east longitude of subplanet point in degrees, positive towards east.

2016 and December 2020. In Table 3 we present the number of stellar occultations predicted by year for each satellite. It is possible to see an increase in the number of events found for Phoebe in 2018 and for the satellites of Jupiter in 2019-2020. This is because at that periods these satellites will cross the apparent galactic plane. In contrast, for Nereid and Triton, almost no occultation was found because Neptune is in a very low dense region of stars and move more slowly than the other planets. We call attention that about 10% (516) of the events will involve stars brighter than magR=14 (and almost 25% brighter than magR=15), which helps the attempt of amateur observers.

Table 4 shows a sample of the catalogue of occultations generated and their parameters, which are necessary to produce occultation maps. Since these objects are very small, the duration of each event is a few seconds. All the occultation tables and maps will be publicly available at the CDS. No star brighter than MagR*=18 will be occulted by Triton in 2016. For this satellite, we cut events with stars fainter than R=18, since for Triton the flux drop during such an occultation would be very small. In Fig. 5 we show an example of an occultation map. This is one of the only two found occultation by Triton and it will happen in October 05, 2017. This event can be observed from Europe and the east coast of USA and will be a great opportunity to study in high resolution the atmosphere of the satellite.

The first preliminary catalogue version of the ESA astrometry satellite GAIA (de Bruijne 2012) is expected to be released up to the end of 2016 (The catalogue with five-parameter astrometric solutions is up to the end of 2017). The precise star positions to be derived by GAIA will provide better predictions with the main source of error being the ephemeris. Astrometric reduction of observations published in Gomes-Júnior et al. (2015) will be revised with the GAIA catalogue and the predictions will be improved. Since we cannot foresee exactly when the GAIA catalogue will be released and when new and re-reduced satellite positions in the GAIA frame will become available, we decided to publish predictions up to the end of 2020. In the GAIA era, the occultation predictions will be updated.

3.1 Prediction test

Observing a stellar occultation demands a great effort. And, in our case, the shadow covers a very restricted area on Earth because of the size of the irregular satellites. Since no stellar occultation by an irregular satellite was observed up to date, with the exception of Triton, and since we want to be sure that we can start observational campaigns with reasonable chances of success, we tested an occultation prediction for a large target, to assess the quality of the prediction.

The test design consisted in observing the object and star to be occulted near the date of the event predicted when the two objects were present in the same field of view (FOV), close to each other. Thus, the relative positions between the two objects had minimal influence of the errors of the reference catalogue of stars used and possible field distortions (Peng et al. 2008, and references therein). The relative positions of the star and satellite were used to check the original predictions. Notice that in the test we do not attempt to observe any actual occultation. The test could be performed at any site, regardless of the Earth location where the occultation would in fact be visible.

We tested the occultation by Himalia predicted to occur on March 3, 2015. The shadow would cross the northern part of South America. For the event, four situations were considered:

(i) Our nominal, published prediction with the STE ephemeris (see Sec. 2), and the nominal UCAC4 position of the star;
(ii) Prediction with the JPL ephemeris and the nominal UCAC4 position of the star;

Table 4. A sample of stellar occultation predictions for Pasiphae

d m Year h m s	RA (ICRS) Dec	C/A	P/A	ν	D	R^*	λ	LST	$\mu_{\alpha*}$	μ_δ
09 04 2016 03:58:19.	11 14 36.7707 +07 39 20.7610	1.003	17.9	-12.88	4.54	14.9	271.	22:03	12.	-33.
13 06 2016 00:16:12.	11 12 48.5020 +07 06 43.3520	0.661	30.0	+14.32	5.50	13.9	262.	17:45	-1.	1.
27 06 2016 13:56:09.	11 18 03.4160 +06 23 45.1940	1.707	28.0	+20.29	5.74	11.7	44.	16:53	4.	-10.
18 07 2016 15:07:24.	11 28 15.5076 +05 05 31.8060	0.942	26.7	+27.80	6.05	14.0	8.	15:40	4.	4.
22 07 2016 16:15:07.	11 30 30.4310 +04 48 43.4340	0.644	206.5	+29.04	6.11	14.6	348.	15:27	23.	-24.
24 07 2016 01:37:34.	11 31 17.8471 +04 42 49.0540	0.029	206.6	+29.46	6.12	15.1	206.	15:22	2.	-8.
24 07 2016 17:37:18.	11 31 40.7472 +04 39 57.5060	0.840	26.5	+29.66	6.13	14.9	326.	15:20	-11.	-1.

Notes. Entries included: day of the year and UTC time of the prediction; right ascension and declination of the occulted star - at the central instant of occultation (corrected by proper motions); C/A: the geocentric closest approach, in arcseconds; P/A: the satellite position angle with respect to the occulted star at C/A, in degrees (zero at north of the star, increasing clockwise); ν: velocity in the plane of sky, in km s^{-1}: positive = prograde, negative = retrograde; D: planet range to Earth, in AU; R^*: normalized magnitude to a common shadow velocity of 20 km s^{-1} by the relationship $\mathrm{R}^* = \mathrm{R}_{\mathrm{actual}} + 2.5 \times \log 10 \left(\frac{\mathrm{velocity}}{20\mathrm{km\,s}^{-1}}\right)$; λ: east longitude of subplanet point in degrees, positive towards east; LST: UT + λ: local solar time at subplanet point, hh:mm; $\mu_{\alpha*}$ and μ_δ: proper motions in right ascension and declination, respectively (mas/year).

(iii) From star and satellite offsets calculated from observations made a few days before the occultation when the objects were very separated (different FOVs);

(iv) Same as 3 but with the star and the satellite close in the same FOV.

Table 5 shows the differences between the predictions in the four situations. For situation 3 we observed the objects on February 22 with the Zeiss telescope (diameter = 0.6m; FOV = 12.′6; pixel scale = 0.″37/*pixel*) at the Observatório do Pico dos Dias, Brazil (OPD, IAU code 874, 45°34′57″W, 22°32′04″S, 1864m). On that day, Himalia and the star were observed in separate FOVs as they were still far apart. On the night of the event, March 3, the objects were observed with Perkin-Elmer telescope (diameter = 1.6m; FOV = 5.′8; pixel scale = 0.″17/*pixel*) at OPD just over an hour after the time scheduled for the event. Satellite and star were separated by about 16 arcsec, so very close to each other (situation 4). From the calculated offsets, the center of the shadow was obtained. Notice that the shadow path was not predicted to cross the OPD (which was located at almost 2000 km south from the shadow path). This was not necessary for testing the prediction.

The critical parameter in the comparisons is the C/A, which here is related to latitudes. The apparent radius of Himalia is about 20 mas (see Table 1). In the context of the test, for a 0 mas offset in C/A we would have 100% probability of observing the occultation, and 0% in the case of a C/A offset equal to or larger than 20 mas, the radius of Himalia. From Table 5, we have nearly 0% probability of success in situation 3, for which the offset in C/A was -20 mas, but when the relative astrometry was poor, 10 days prior to the event. Once at the day of the event in situation 4, the C/A offset dropped to -9 mas only, corresponding to a 55% probability of success. Comparison with the prediction using the JPL ephemeris (situation 2) gives a +11 mas C/A offset, or a compatibility of 45% between the ephemerides. All this suggests that there was a good probability of observing the event. The largest differences between the shadows of the four situations were 36s in time along the shadow path and 101km (31 mas) in the direction perpendicular to the shadows, suggesting that observers should be spread in narrow latitude ranges 100 km wide.

Table 5. Comparison between the predictions of the Himalia occultation at March 03, 2015.

Differences with respect to the STE prediction			
Method	Instant of C/A	C/A	Sit.
STE	00:39:51 UTC	0.″703	i
JPL	-26s	+11mas (36km)	ii
Feb. 22 Obs.	-14s	-20mas (65km)	iii
Mar. 03 Obs.	-36s	-09mas (29km)	iv

C/A: geocentric closest approach; Sit: Situation test considered.

4 DISCUSSION

We predict stellar occultations for the period of 2016-2020 for eight irregular satellites of Jupiter: Ananke, Carme, Elara, Himalia, Leda, Lysithea, Pasiphae, and Sinope; one satellite of Saturn: Phoebe; and two satellites of Neptune: Triton and Nereid. The procedure used was the same as that for the prediction of stellar occultations by Pluto and its satellites in Assafin et al. (2010) and by Centaurs and TNOs in Assafin et al. (2012) and Camargo et al. (2014).

For this, we generated new numerical integration of the orbits of the irregular satellites of Jupiter. A specific short-time ephemeris were obtained using only the positions of Gomes-Júnior et al. (2015). The systematic errors found in the JPL ephemeris (Jacobson et al. 2012) were corrected. We also updated the ephemeris of Desmars et al. (2013) using the observations of Gomes-Júnior et al. (2015), from MPC and from Flagstaff. For Nereid and Triton we used the most recent ephemeris available (Emelyanov & Arlot 2011; Emelyanov & Samorodov 2015, , respectively).

The candidate stars were searched in the UCAC4 catalogue, except for the candidates in 2016 for Triton and Nereid. In this case, we used the WFI catalogue that was generated from observations made with ESO2p2/WFI CCD mosaic that covered the path of Neptune in the sky-plane

up to 2016 (see Sec. 3). From this, a total of 5457 events are foreseen.

In a broader, general sense, the probability of successfully observing an occultation is roughly the ratio of the satellite's radius by the budget error (2 sigma for a 95% confidence level) of ephemeris and star position. Thus, UCAC4 errors ranging between 20 mas - 50 mas (1 sigma) combined with a mean error (1 sigma) in the JPL ephemeris of 30 mas for Himalia and 150 mas for Leda published in Table 2 of Jacobson et al. (2012) would give 28%-17% probability of observing such an event by Himalia and $\approx 2\%$ for Leda, the smallest irregular satellite in the sample. Observations a few days before the date of occultation predicted may improve the combined errors to 40-80 mas, depending on the magnitude of the objects.

The test made with an occultation expected to happen in March 03, 2015 for Himalia showed that this event would probably have been observed successfully in case there were observers available in the shadow area. The results show satisfying small offsets with respect to the local of the prediction.

Continuous observations of the satellites are recommended and fitting of our dynamical model to those observations are expected to reduce the respective STE ephemeris errors. The first version of the GAIA catalogue is to be released up to the end of 2016 and will improve the position error of the stars to the 1-5 mas level. It will allow for the discovery of ocultations by fainter stars not present in the UCAC4 catalogue. The release of the GAIA catalogue should have a positive impact on both the astrometric precision of occulted stars and the reduction of astrometric positions of the satellites. As a result, prediction of stellar occultations by irregular satellites shall increase in number as well as in success.

ACKNOWLEDGEMENTS

ARG-J thanks the financial support of CAPES. MA thanks the CNPq (Grants 473002/2013-2 and 308721/2011-0) and FAPERJ (Grant E-26/111.488/2013). RV-M thanks grants: CNPq-306885/2013, Capes/Cofecub-2506/2015, Faperj/PAPDRJ-45/2013. JIBC acknowledges CNPq for a PQ2 fellowship (process number 308489/2013-6). BEM thanks the financial support of CAPES. FB-R acknowledges PAPDRJ-FAPERJ/CAPES E-43/2013 number 144997, E-26/101.375/2014. The numerical model of the satellites of Jupiter was developped during a post-doctoral contract funded by the Chinese Academy of Sciences (CAS) and supported by the National Scientific Fund of China (NSFC)

References

Agnor C. B., Hamilton D. P., 2006, Nature, 441, 192–194

Assafin M., Camargo J. I. B., Vieira Martins R., Andrei A. H., Sicardy B., Young L., da Silva Neto D. N., Braga-Ribas F., 2010, Astronomy & Astrophysics, 515, A32

Assafin M., Camargo J. I. B., Vieira Martins R., Braga-Ribas F., Sicardy B., Andrei A. H., da Silva Neto D. N., 2012, Astronomy & Astrophysics, 541, A142

Assafin M., Vieira Martins R., Camargo J. I. B., Andrei A. H., Da Silva Neto D. N., Braga-Ribas F., 2011, in Tanga P., Thuillot W., eds, Gaia follow-up network for the solar system objects : Gaia FUN-SSO workshop proceedings, held at IMCCE -Paris Observatory, France, November 29 - December 1, 2010. ISBN 2-910015-63-7 PRAIA - Platform for Reduction of Astronomical Images Automatically. pp 85–88

Barucci M. A., Brown M. E., Emery J. P., 2008, Composition and Surface Properties of Transneptunian Objects and Centaurs. Barucci, M. A. and Boehnhardt, H. and Cruikshank, D. P. and Morbidelli, A. and Dotson, R., pp 143–160

Braga-Ribas F., Sicardy B., Ortiz J. L., Lellouch E., Tancredi G., Lecacheux J., Vieira-Martins R., Camargo J. I. B., Assafin M., Behrend R., et al., 2013, ApJ, 773, 26

Braga-Ribas F., Sicardy B., Ortiz J. L., Snodgrass C., Roques F., Vieira-Martins R., Camargo J. I. B., Assafin M., Duffard R., Jehin E., et al., 2014, Nature, 508, 72–75

Camargo J. I. B., Vieira-Martins R., Assafin M., Braga-Ribas F., Sicardy B., Desmars J., Andrei A. H., Benedetti-Rossi G., Dias-Oliveira A., 2014, Astronomy & Astrophysics, 561, A37

Clark R. N., Brown R. H., Jaumann R., Cruikshank D. P., Nelson R. M., Buratti B. J., McCord T. B., Lunine J., Baines K. H., Bellucci G., et al. 2005, Nature, 435, 66–69

de Bruijne J. H. J., 2012, Astrophysics and Space Science, 341, 31–41

Desmars J., Li S. N., Tajeddine R., Peng Q. Y., Tang Z. H., 2013, Astronomy & Astrophysics, 553, A36

Elliot J., Person M. J., McDonald S. W., Buie M. W., Dunham E. W., Millis R. L., Nye R. A., Olkin C. B., Wasserman L. H., Young L., Hubbard W. B., Hill R., Reitsema H. J., Pasachoff J. M., McConnochie T. H., Babcock B. A., Stone R. C., Francis P., 2000, Icarus, 148, 347–369

Elliot J. L., Person M. J., Zuluaga C. A., Bosh A. S., Adams E. R., Brothers T. C., Gulbis A. A. S., Levine S. E., Lockhart M., Zangari A. M., et al. 2010, Nature, 465, 897–900

Emelyanov N. V., Arlot J.-E., 2011, Monthly Notices of the Royal Astronomical Society, 417, 458–463

Emelyanov N. V., Samorodov M. Y., , 2015, Analytical theory of motion and new ephemeris of Triton from observations

Emel'yanov N. V., Arlot J.-E., 2008, Astronomy and Astrophysics, 487, 759–765

Everhart E., 1985, in Carusi A., Valsecchi G. B., eds, Dynamics of Comets: Their Origin and Evolution, Proceedings of IAU Colloq. 83, held in Rome, Italy, June 11-15, 1984. Edited by Andrea Carusi and Giovanni B. Valsecchi. Dordrecht: Reidel, Astrophysics and Space Science Library. Volume 115, 1985, p.185 An efficient integrator that uses Gauss-Radau spacings. p. 185

Gomes-Júnior A. R., Assafin M., Vieira-Martins R., Arlot J.-E., Camargo J. I. B., Braga-Ribas F., da Silva Neto D. N., Andrei A. H., Dias-Oliveira A., Morgado B. E., et al. 2015, Astronomy & Astrophysics

Grav T., Bauer J., 2007, Icarus, 191, 267–285

Grav T., Holman M. J., Gladman B. J., Aksnes K., 2003, Icarus, 166, 33–45

Jacobson R., Brozović M., Gladman B., Alexandersen M., Nicholson P. D., Veillet C., 2012, The Astronomical Journal, 144, 132

Jacobson R. A., 2009, The Astronomical Journal, 137, 4322–4329
Jewitt D., Haghighipour N., 2007, Annual Review of Astronomy and Astrophysics, 45, 261–295
Johnson T. V., Lunine J. I., 2005, Nature, 435, 69–71
Lainey V., Duriez L., Vienne A., 2004, Astronomy and Astrophysics, 420, 1171–1183
McKinnon W., Kirk R., 2007, Encyclopedia of the Solar System, p. 483–502
Olkin C., Elliot J., Hammel H., Cooray A., McDonald S., Foust J., Bosh A., Buie M., Millis R., Wasserman L., et al., 1997, Icarus, 129, 178–201
Ortiz J. L., Sicardy B., Braga-Ribas F., Alvarez-Candal A., Lellouch E., Duffard R., Pinilla-Alonso N., Ivanov V. D., Littlefair S. P., Camargo J. I. B., et al. 2012, Nature, 491, 566–569
Peng Q., Vienne A., Lainey V., Noyelles B., 2008, Planetary and Space Science, 56, 1807–1811
Peng Q. Y., Wang N., Vienne A., Zhang Q. F., Li Z., Meng X. H., 2015, Monthly Notices of the Royal Astronomical Society, 449, 2638–2642
Porco C. C., West R. A., McEwen A., Del Genio A. D., Ingersoll A. P., Thomas P., Squyres S., Dones L., et al., 2003, Science, 299, 1541–1547
Rettig T., Walsh K., Consolmagno G., 2001, Icarus, 154, 313–320
Sheppard S. S., 2005, in Asteroids, Comets, Meteors Vol. 1 of Proceedings of the International Astronomical Union, Outer irregular satellites of the planets and their relationship with asteroids, comets and kuiper belt objects. pp 319–334
Sicardy B., Ortiz J. L., Assafin M., Jehin E., Maury A., Lellouch E., Hutton R. G., Braga-Ribas F., Colas F., Hestroffer D., et al. 2011, Nature, 478, 493–496
Thomas P., 2000, Icarus, 148, 587–588
Thomas P., 2010, Icarus, 208, 395–401
Thomas P., Veverka J., Helfenstein P., 1991, J. Geophys. Res., 96, 19253
U.S.N.O, 2015, Flagstaff Astrometric Scanning Transit Telescope Planet and Planetary Satellite Observations
Zacharias N., Finch C. T., Girard T. M., Henden A., Bartlett J. L., Monet D. G., Zacharias M. I., 2013, The Astronomical Journal, 145, 44
Zhang H. Y., Shen K. X., Dourneau G., Harper D., Qiao R. C., Xi X. J., Cheng X., Yan D., Li S. N., Wang S. H., 2014, Monthly Notices of the Royal Astronomical Society, 438, 1663–1668
Ćuk M., Burns J. A., 2004, Icarus, 167, 369–381